

A statistical exploration of multiple exciton generation in silicon quantum dots and optoelectronic application

W. A. Su and W. Z. Shen

Citation: *Appl. Phys. Lett.* **100**, 071111 (2012); doi: 10.1063/1.3687184

View online: <http://dx.doi.org/10.1063/1.3687184>

View Table of Contents: <http://apl.aip.org/resource/1/APPLAB/v100/i7>

Published by the [American Institute of Physics](#).

Related Articles

Non-Hermitian exciton dynamics in a photosynthetic unit system

JCP: BioChem. Phys. **6**, 02B609 (2012)

Non-Hermitian exciton dynamics in a photosynthetic unit system

J. Chem. Phys. **136**, 065104 (2012)

Resonantly enhanced optical nonlinearity in hybrid semiconductor quantum dot–metal nanoparticle structures

Appl. Phys. Lett. **100**, 063117 (2012)

Two-dimensional electrostatic lattices for indirect excitons

Appl. Phys. Lett. **100**, 061103 (2012)

Observation of quantum beat oscillations and ultrafast relaxation of excitons confined in GaAs thin films by controlling probe laser pulses

J. Appl. Phys. **111**, 023505 (2012)

Additional information on *Appl. Phys. Lett.*

Journal Homepage: <http://apl.aip.org/>

Journal Information: http://apl.aip.org/about/about_the_journal

Top downloads: http://apl.aip.org/features/most_downloaded

Information for Authors: <http://apl.aip.org/authors>

ADVERTISEMENT

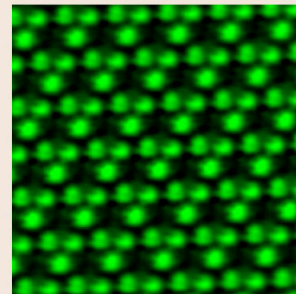
The Asylum Research logo is shown, featuring the company name in a stylized font with a blue and white color scheme. Below the logo, the tagline "The Technology Leader in SPM/AFM" is written.

Register Now at
www.asylumresearch.com

Free AFM Webinar February 22 Register Now

"Smaller and Quieter: Ultra-High Resolution AFM Imaging"

With Jason Cleveland, AFM pioneer,
inventor and Asylum Research co-founder



A statistical exploration of multiple exciton generation in silicon quantum dots and optoelectronic application

W. A. Su and W. Z. Shen^{a)}

Laboratory of Condensed Matter Spectroscopy and Opto-Electronic Physics, Key Laboratory of Artificial Structures and Quantum Control (Ministry of Education), Department of Physics, and Institute of Solar Energy, Shanghai Jiao Tong University, 800 Dong Chuan Road, Shanghai 200240, China

(Received 18 December 2011; accepted 31 January 2012; published online 17 February 2012)

We have carried out an investigation of multiple exciton generation (MEG) in Si quantum dots (QDs) and its application in optoelectronic devices. A simple yet effective statistical model has been proposed based on Fermi statistical theory and impact ionization mechanism. It is demonstrated that the MEG efficiency depends on both the radius of Si QDs and the energy of incident photons, with the MEG threshold energy in the range of ~ 2.2 – $3.1 E_g$ depending on the dot radius. While limited improvement has been observed in power conversion efficiency of single stage solar cells, MEG in Si QDs exhibits prospective for application in ultraviolet detectors due to the high internal quantum efficiency under short incident light. © 2012 American Institute of Physics. [doi:10.1063/1.3687184]

Semiconductor nanocrystals have attracted a great deal of attention for potential application in photonics,¹ medicine,² and solid state optoelectronic devices.^{3,4} In particular the observation of multiple exciton generation (MEG) has drawn considerable interest, since it offers prospects for the development of high-efficient solar cells,^{3,5–9} high-sensitive photodetectors,⁴ high-quality optical amplifiers,¹⁰ and high-performance lasers,^{10,11} as well as avalanche photodiodes.^{12,13} MEG can occur when absorbing a high energy photon leads to generate two or more excited electron-hole pairs with photon energy at least equal to or greater than two times the semiconductor nanocrystals band gap, E_g . In this case, the excess energy is used to excite a second electron across the band gap instead of dissipated as heat through sequential phonon emission. The analogous phenomenon of multiple charge carrier generation per photon in bulk semiconductors is termed carrier multiplication and is explained in terms of impact ionization. MEG in semiconductor nanocrystals can also be explained by the more conventional impact ionization mechanism,¹⁴ whereby a photogenerated electron-hole pair decays into a biexciton in a process driven by Coulomb interactions between the carriers.¹⁵

The high efficient MEG in PbSe nanocrystals was reported in 2004.⁹ Since then, the occurrence of MEG has been observed for PbSe,^{9,16–21} PbS,^{17,19} PbTe,²² CdSe,¹⁸ CdTe,^{23,24} Si,²⁵ and InAs (Ref. 26) quantum dots (QDs). The most popular materials of MEG investigated is group IV–VI (PbSe, PbS) QDs. Silicon semiconductor technology not only stands as the foundation of today's widely manufactured integrated circuit technology but also comprises more than 90% of the current photovoltaic cell production. However, only MEG effect in colloidal Si QDs (Ref. 25) and MEG enhanced luminescence quantum yield in Si nanocrystals²⁷ have been reported so far. It is significative for further comprehensive investigation of MEG in Si QDs and its

applications. The present work involves MEG in Si QDs and its application in optoelectronic devices. A simple yet effective statistical model, based on Fermi statistical theory²⁸ and impact ionization mechanism,¹⁴ has been proposed to investigate the effects of MEG in semiconductor QDs. We have shown that, in contrast to the limited improvement in power conversion efficiency of single stage solar cells, MEG in Si QDs is likely prospective for its application in ultraviolet detectors due to the high internal quantum efficiency under short incident light.

A great number of experimental^{29–32} and theoretical studies^{32–36} have been done to clarify the quantum confinement effects in Si nanocrystals. However, no consensus has been achieved on the formula of E_g vs diameter of silicon nanocrystals due partly to the variety and complexity of the samples studied. It seems to be of prime importance to perform reliable but simple determination of the size dependence of E_g . By fitting of experimental and theoretical data^{29–36} (as shown in Fig. 1), an empirical formula has been established that represents the relationship between E_g (eV) and diameter d (nm) of Si nanocrystals, which can be expressed as,

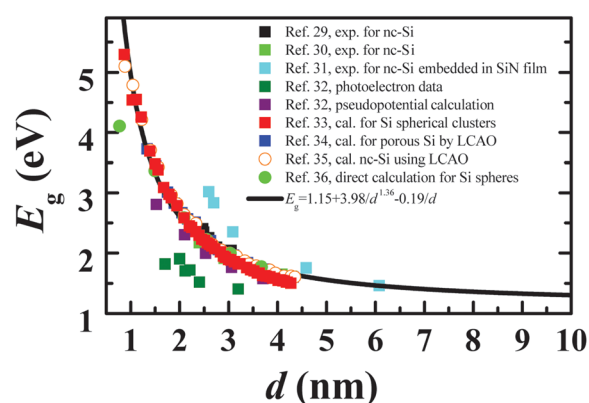


FIG. 1. (Color online) Bandgap energy E_g of silicon nanocrystals as a function of crystal size d .

^{a)} Author to whom correspondence should be addressed. Electronic mail: wzshen@sjtu.edu.cn.

$$E_g = 1.15 + \frac{3.98}{d^{1.36}} - \frac{0.19}{d}, \quad (1)$$

The fitted value 1.15 eV is the bulk band gap of Si and agrees very well with that reported in the literature.^{37,38} Equation (1) reveals the spatial localization of the electron and hole following approximately a $d^{-1.36}$ law. This finding is in agreement with results of $d^{-1.39}$ and $d^{-1.37}$ law^{35,36} but differs from the result of effective mass approximation which expects a d^{-2} law.³⁹ The lower exponent 1.36 shows that the exact nature of the bands,^{35,36} possible surface effects and structural changes³⁹ have to be taken into account. Equation (1) also indicates the size dependent Coulomb attraction increasing as d^{-1} . We have depicted the calculated size dependent E_g of Si QDs as solid curve in Fig. 1. Obviously, it agrees very well with most of the experimental and theoretical data. Therefore, Eq. (1) should also well describe for the plasma-synthesized Si QDs that have been used in Ref. 25, on which our model is optimized below.

In semiconductor QDs of the band gap E_g , the absorption of a single photon of high-energy $h\nu \geq nE_g$ (h is the Planck constant and ν photon frequency) may generate m ($m \leq n$) electron-hole pairs due to impact ionization.¹⁴ In this process, the incident photon energy is released into the energy relaxation volume Ω (a volume within which electron-hole pairs are generated) of QDs for an ultra-short time t_s amount to 50–200 fs,⁴⁰ leading to a statistical equilibrium final state with $2m$ particles. On the other hand, crystal momentum need not be conserved because momentum is not a good quantum number for three-dimensionally confined carriers. This multiple exciton generation process is similar to that of multiple elementary particles formation Fermi dealt with²⁸ and it has been demonstrated recently that the statistical method can be used to explore MEG in semiconductor QDs.⁴¹ According to Fermi statistical theory,²⁸ the statistical weight $\omega(2m)$ can be expressed as,

$$\omega(2m) = 2 \times \frac{(m_n^* m_p^*)^{3m/2} \Omega^{2m}}{2^{3m} \pi^{3m} \hbar^{6m}} \frac{(h\nu - mE_g)^{3m-1}}{(3m-1)!}, \quad (2)$$

where the electron spin has been taken into account with $\hbar = h/2\pi$ and $m_{n,p}^*$ the effective masses of electron and hole, respectively.

The maximum number of electron-hole pairs M is equal to $[h\nu/E_g]$, where the square bracket denotes the integer part of $h\nu/E_g$, and the statistical average number of electron-hole pairs $\langle N_{exc} \rangle$ can be calculated by,

$$\langle N_{exc} \rangle = \frac{\sum_{m=1}^M m \omega(2m)}{\sum_{m=1}^M \omega(2m)}. \quad (3)$$

Since the MEG efficiency I_{QE} is the inner quantum efficiency in semiconductor materials which is usually defined as the average number of electron-hole pairs created by the absorption of a single photon,⁴² it can be expressed as,

$$I_{QE} = \langle N_{exc} \rangle \times 100\%. \quad (4)$$

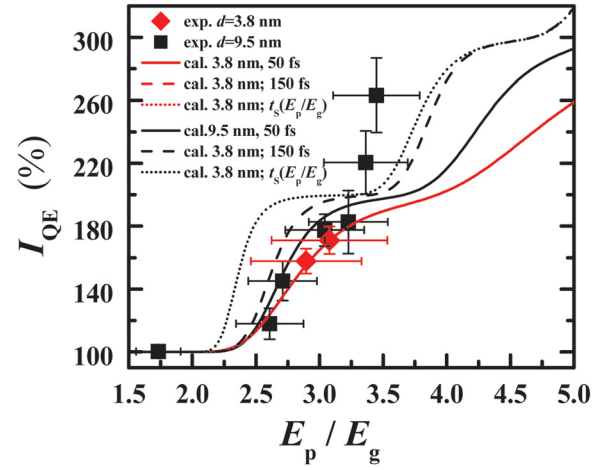


FIG. 2. (Color online) MEG efficiency I_{QE} in Si QDs as a function of incident photon energy E_p . Red diamonds and black squares are experimental MEG efficiencies for 3.8 and 9.5 nm Si QDs, respectively, taken from Ref. 25. Curves are the calculated MEG efficiency from our model, see text for details.

It should be noted that the optical selection rules have not been included in the proposed statistical model due to the non-conservation of the crystal momentum in low-dimensional materials. The model is therefore unsuitable for bulk Si.

For justifying the proposed statistical model, we first perform the theoretical calculation of MEG efficiency I_{QE} for Si QDs with average diameters of 3.8 and 9.5 nm to make a direct comparison with the reported experimental MEG efficiency.²⁵ A log normal distribution size of Si QDs with a standard deviation of 15% has also been taken into account in the calculation, together with $m_n^* = 0.190 m_0$ and $m_p^* = 0.286 m_0$ (m_0 is the electron vacuum mass).³⁷ As shown in Fig. 2, the calculated MEG efficiency I_{QE} at a characteristic time $t_s = 50$ fs are found to agree basically with the experimental data of 3.8 and 9.5 nm Si QDs under different incident photon energies E_p . However, it is clear that the experimental MEG efficiencies in the 9.5 nm Si QDs are much larger than the theoretical results at high incident photon energies ($E_p > 3.3 E_g$).

As we know, t_s describes the characteristic time for the incident photon energy released into QDs, and should

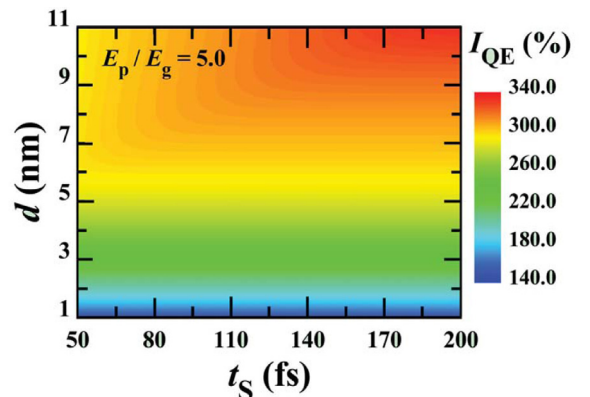


FIG. 3. (Color online) Calculated MEG efficiency I_{QE} for Si QDs as a function of diameter d and characteristic time t_s . Incident photon energy E_p fixed at five times of E_g .

depend on the photon energy E_P . Fig. 3 presents the detailed calculation of the MEG efficiency I_{QE} as functions of t_S and d . For a given incident photon energy, the MEG efficiency I_{QE} has demonstrated to be strongly depend on t_S for large (>6.0 nm) Si QDs, while it is almost independent of t_S for small dots. We have employed another characteristic time $t_S = 150$ fs to re-calculate the MEG efficiency I_{QE} for the 9.5 nm Si QDs (black dot curve in Fig. 2), where a better agreement with the experimental data has been achieved at high incident photon energies, but fails at low incident photon ones. This conflict reveals that the characteristic time t_S does depend on E_P .

Impact ionization process is similar to that of hot-electron cooling in QDs (Ref. 43) since both are energy releasing process through multiple particles generation, and the relaxation time for the latter is found to have an exponential form.⁴³ Considering the spatial confinement for the generation of multiple electron-hole pairs in QDs through impact ionization, we can therefore assume the relationship of the characteristic time t_S in terms of normalized incident photon energy E_P/E_g as $t_S(E_P/E_g) = 35.0 + 3.0 \times 10^{-9} \cdot \exp[21.0(E_P/E_g)^{1/10}]$ fs. The black dash curve in Fig. 2 is the calculated MEG efficiency I_{QE} for the 9.5 nm Si QDs with the photon energy-dependent characteristic time $t_S(E_P/E_g)$. It is clear that the calculated MEG efficiency I_{QE} agrees well with the reported experimental data in Si QDs (Ref. 25) over a wide range of incident photon energies. We have also calculated the MEG efficiency I_{QE} for the 3.8 nm Si QDs with $t_S(E_P/E_g)$, and have found that the result is identical to the calculation with $t_S = 50$ and 150 fs (these three curves are actually identical in Fig. 2). This comparison demonstrates that the present statistical model with the photon energy-dependent characteristic time is able to explore the MEG effect in Si QDs.

We now employ the established reliable model to explore the MEG efficiency in Si QDs. Fig. 4 shows the determined dependence of the MEG efficiency I_{QE} on d , E_P/E_g and $t_S(E_P/E_g)$. It reveals that, for a given QD size, the initially constant value of the MEG efficiency for the lower incident photon energies is followed by an increase for larger photon energies. This observation has been widely reported in the experimental studies^{9,16-19,40,44,45} and can be easily

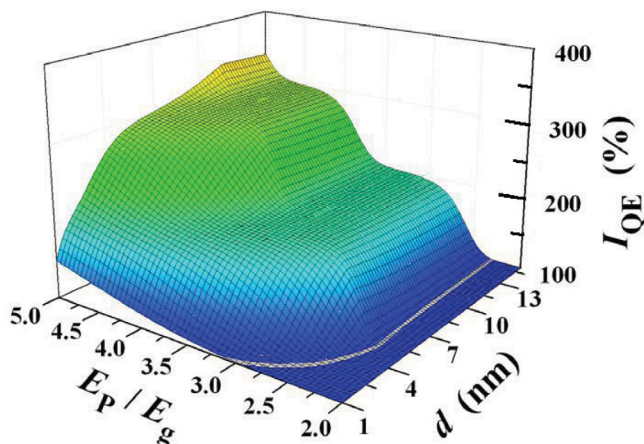


FIG. 4. (Color online) Calculated MEG efficiency I_{QE} for Si QDs as a function of diameter d and normalized incident photon energy E_P/E_g . Gray band is the threshold energy E_T for MEG in various Si QDs.

understood in the light of the fact that an incident photon with higher energy can generate more electron-hole pairs. One can further observe a very specific common step-like character of the MEG efficiency I_{QE} in the higher energy range for larger Si QDs ($d > \sim 3.0$ nm), which is also existed in Fig. 2. The MEG efficiency “steps” coincide with the integral MEG efficiency I_{QE} , i.e., the generation of electron-hole pairs multiplied by two and three. The occurrence of the MEG efficiency “steps” in Si QDs is due to the fact that the number of electron-hole pairs generated in a Si QD through absorbing a photon must be integral. The step-like increase in the MEG efficiency for larger incident photon energies has been theoretically^{19,46} and experimentally^{13,27} reported and seen as the most characteristic fingerprint of the MEG process.

On the other hand, Fig. 4 also presents that, for a given incident light E_P/E_g , the MEG efficiency I_{QE} in Si QDs enhances rapidly and then reaches constant values in the case of “steps” with the increase of dot size. This behavior can be well understood from the effect of the quantum confinement in Si QDs. According to Kayanuma,⁴⁷ the quantum confinement will be very strong in the range of less than 2 times the exciton Bohr radius a_B (for Si, $a_B = 4.9$ nm), while it becomes weak in the range of larger than $4a_B$. All Si QDs we calculated have the quantum confinement effect which leads to Coulomb interaction enhancement and final states density discretization. It is well known that the MEG effect depends on both the Coulomb interaction and the density of final states.^{45,48} In QDs, the enhanced Coulomb interaction would lead to higher MEG efficiency,^{9,49} while the density of final states is reduced because of the discretization of the states. The Coulomb attraction increases as d^{-1} and the energy of spatial localization, which origins from the discretization of the states,⁵⁰ enhances as $d^{-1.36}$ for both electrons and holes [see Eq. (1)]. The density of states in QDs with small sizes reduce drastically with the radius, leading to the dominance of the final states density discretization over the Coulomb attraction, and therefore the MEG efficiency I_{QE} in Si QDs increases rapidly with the dot size for small sizes.

In addition to the MEG efficiency, another important characteristic is the MEG threshold energy E_T , which is the minimum photon energy $h\nu'$ necessary to achieve MEG in QDs. We can numerically calculate the MEG threshold energy E_T by using $I_{QE} = I_{QE,cr}(d, h\nu')$, where $I_{QE,cr}(d, h\nu')$ is the criterion for MEG occurring in Si QDs. The gray band in Fig. 4 is a d -dependent E_T , obtained by using the criterion $I_{QE,cr}(d, h\nu') = 101.0\%$ at various fixed d s. It is clear that E_T depends significantly on the Si QD size, exhibiting first rapid decrease and then slight increase in the examined diameter d from 1.0 to 15.0 nm with the minimum E_T of $2.2 E_g$ at $d = 5.2$ nm. The calculated E_T ranges from ~ 2.2 to $3.1 E_g$ and the value for 9.5 nm Si QDs is $\sim 2.3 E_g$, which is in good agreement with the reported result of $2.4 \pm 0.1 E_g$ in the literature.²⁵

We finally explore the potential application of MEG in Si nanocrystals for optoelectronic devices. Fig. 5(a) shows the calculated power conversion efficiency for a single stage solar cells based on a single size Si QDs, for one without MEG, for one with MEG obtained by the present reliable model, and for one with ideal MEG (i.e., ideal “staircase”

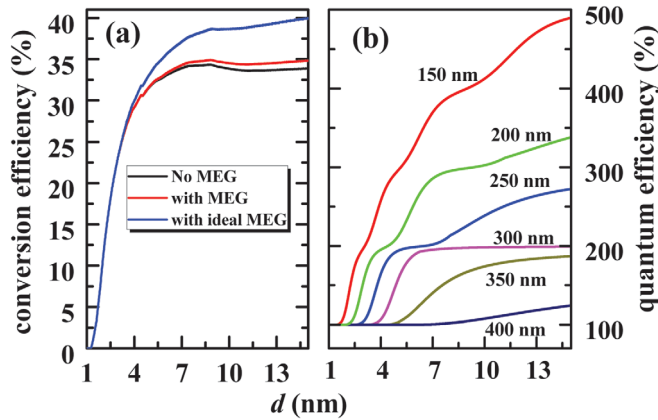


FIG. 5. (Color online) (a) Calculated power conversion efficiencies of single stage Si QDs solar cells as a function of dots diameter d at solar spectra AM1.5 G, and (b) Dependence of the internal quantum efficiency on the Si QD diameter d and incident light wavelength, both with the photon energy-dependent characteristic time $t_s(E_p/E_g)$.

profiles for MEG quantum efficiency).^{51,52} All calculations follow the detailed balance model of Shockley and Queisser⁵³ under 1-sun AM1.5 G solar spectrum with the cell temperature at 300 K. MEG is incorporated into the calculations through the energy-dependent quantum efficiency $I_{QE,cr}(d, h\nu)$. We note that the power conversion efficiency for single stage Si QDs solar cells first increases with d and then almost unchanged. The power conversion efficiency can be improved by the MEG effect only for large size Si QDs ($d > \sim 5.0$ nm) and the value for $d > 10.0$ nm is increased by $\sim 1\%$ although it can be enhanced by $\sim 5\%$ for the ideal MEG case. As we know, the power conversion efficiency is determined by the overlap of the solar photon flux spectrum and the semiconductor material's quantum efficiency. With the increase of Si QD size, the energy band gap decreases, resulting in the relatively larger overlap and therefore the higher power conversion efficiency. The very small (up to only 1%) improvement in the power conversion efficiency of a single stage Si QDs solar cells by MEG is simply due to the large energy band gap (>1.15 eV) and high threshold energy ($E_T \sim 2.2\text{--}3.1 E_g$) in Si QDs.

Though application of MEG in Si QDs is not very prospective for solar cells, it is likely to provide significant benefits for the property of ultraviolet detectors. Fig. 5(b) illustrates the internal quantum efficiency of Si QDs detectors under different incident light wavelengths. It demonstrates that the internal quantum efficiency of Si QDs is evident under ultraviolet incident light and the internal quantum efficiency can be as high as 490% for Si QDs under 150 nm incident light. The significant benefit comes from the fact that the spectral current responsivity and the ultimate level of sensitivity for ultraviolet detectors have been solely determined by the material's quantum efficiency.⁵⁴

In summary, a simple and effective statistical model has been proposed to explore the MEG effect in Si QDs. After the demonstration of the present model through good agreement with the experimental MEG data for colloidal Si QDs, we have carried out a detailed investigation of the MEG efficiency and threshold energy in various Si QDs with a photon energy-dependent characteristic time $t_s(E_p/E_g)$. We have

shown that the MEG effect in Si QDs can improve only $\sim 1\%$ of the power conversion efficiency for single stage solar cells as a result of large energy band gap (>1.15 eV) and high threshold energy ($E_T \sim 2.2\text{--}3.1 E_g$), however, MEG in Si QDs is likely more prospective for its application in ultraviolet detectors due to the high internal quantum efficiency under short incident light.

This work was supported by the National Major Basic Research Project of 2012CB934302 and the Natural Science Foundation of China under contract 11074169.

- ¹L. Pavesi, L. Negro, C. Mazzoleni, G. Franzo, and F. Priolo, *Nature* **408**, 440 (2000).
- ²J. H. Park, L. Gu, G. von Maltzahn, E. Ruoslahti, S. N. Bhatia, and M. J. Sailor, *Nat. Mater.* **8**, 331 (2009).
- ³D. Timmerman, I. Izuddin, P. Stallings, I. N. Yassievich, and T. Gregorkiewicz, *Nat. Photonics* **2**, 105 (2008).
- ⁴V. Sukhovatkin, S. Hinds, L. Brzozowski, and E. H. Sargent, *Science* **324**, 1542 (2009).
- ⁵V. I. Klimov, *Appl. Phys. Lett.* **89**, 123118 (2006).
- ⁶A. Luque, A. Marti, and A. J. Nozik, *MRS Bull.* **32**, 236 (2007).
- ⁷H. W. Hillhouse and M. C. Beard, *Curr. Opin. Colloid. Interface Sci.* **14**, 245 (2009).
- ⁸J. Sambur, T. Novet, and B. Parkinson, *Science* **330**, 63 (2010).
- ⁹R. D. Schaller and V. I. Klimov, *Phys. Rev. Lett.* **92**, 186601 (2004).
- ¹⁰R. D. Schaller, M. A. Petruska, and V. I. Klimov, *J. Phys. Chem. B* **107**, 13765 (2003).
- ¹¹V. Klimov, A. Mikhailovsky, S. Xu, A. Malko, J. Hollingsworth, C. Leathardale, H. Eisler, and M. Bawendi, *Science* **290**, 314 (2000).
- ¹²B. Kochman, A. D. Stiff-Roberts, S. Chakrabarti, J. D. Phillips, S. Krishna, J. Singh, and P. Bhattacharya, *IEEE J. Quantum Electron.* **39**, 459 (2003).
- ¹³N. M. Gabor, Z. Zhong, K. Bosnick, J. Park, and P. L. McEuen, *Science* **325**, 1367 (2009).
- ¹⁴J. J. H. Pijpers, R. Ulbricht, K. J. Tielrooij, A. Osherov, Y. Golan, C. Delerue, G. Allan, and M. Bonn, *Nat. Phys.* **5**, 811 (2009).
- ¹⁵A. Franceschetti, J. M. An, and A. Zunger, *Nano Lett.* **6**, 2191 (2006).
- ¹⁶M. B. Ji, S. Park, S. T. Connor, T. Mokari, Y. Cui, and K. J. Gaffney, *Nano Lett.* **9**, 1217 (2009).
- ¹⁷R. J. Ellingson, M. C. Beard, J. C. Johnson, P. R. Yu, O. I. Micic, A. J. Nozik, A. Shabaev, and A. L. Efros, *Nano Lett.* **5**, 865 (2005).
- ¹⁸R. D. Schaller, M. A. Petruska, and V. I. Klimov, *Appl. Phys. Lett.* **87**, 253102 (2005).
- ¹⁹R. D. Schaller, M. Sykora, J. M. Pietryga, and V. I. Klimov, *Nano Lett.* **6**, 424 (2006).
- ²⁰J. M. Luther, M. C. Beard, Q. Song, M. Law, R. J. Ellingson, and A. J. Nozik, *Nano Lett.* **7**, 1779 (2007).
- ²¹S. J. Kim, W. J. Kim, Y. Sahoo, A. N. Cartwright, and P. N. Prasad, *Appl. Phys. Lett.* **92**, 031107 (2008).
- ²²J. E. Murphy, M. C. Beard, A. G. Norman, S. P. Ahrenkiel, J. C. Johnson, P. Yu, O. I. Micic, R. J. Ellingson, and A. J. Nozik, *J. Am. Chem. Soc.* **128**, 3241 (2006).
- ²³D. Gachet, A. Avidan, I. Pinkas, and D. Oron, *Nano Lett.* **10**, 164 (2010).
- ²⁴Y. Kobayashi, T. Udagawa, and N. Tamai, *Chem. Lett.* **38**, 830 (2009).
- ²⁵M. C. Beard, K. P. Knutsen, P. R. Yu, J. M. Luther, Q. Song, W. K. Metzger, R. J. Ellingson, and A. J. Nozik, *Nano Lett.* **7**, 2506 (2007).
- ²⁶R. D. Schaller, J. M. Pietryga, and V. I. Klimov, *Nano Lett.* **7**, 3469 (2007).
- ²⁷D. Timmerman, J. Valenta, K. Dohnalova, W. D. A. M. de Boer, and T. Gregorkiewicz, *Nat. Nanotechnol.* **6**, 710 (2011).
- ²⁸E. Fermi, *Prog. Theor. Phys.* **5**, 570 (1950).
- ²⁹S. Furukawa and T. Miyasato, *Phys. Rev. B* **38**, 5726 (1988).
- ³⁰J. von Behren, T. van Buuren, M. Zacharias, E. H. Chimowitz, and P. M. Fauchet, *Solid State Commun.* **105**, 317 (1998).
- ³¹T. Kim, N. Park, K. Kim, G. Sung, Y. Ok, T. Seong, and C. Choi, *Appl. Phys. Lett.* **85**, 5355 (2004).
- ³²T. Van Buuren, L. Dinh, L. Chase, W. Siekhaus, and L. Terminello, *Phys. Rev. Lett.* **80**, 3803 (1998).
- ³³C. Delerue, G. Allan, and M. Lannoo, *J. Lumin.* **80**, 65 (1998).
- ³⁴Q. Zhang and S. Bayliss, *J. Appl. Phys.* **79**, 1351 (1996).
- ³⁵J. P. Proot, C. Delerue, and G. Allan, *Appl. Phys. Lett.* **61**, 1948 (1992).
- ³⁶L. W. Wang and A. Zunger, *J. Phys. Chem.* **98**, 2158 (1994).

- ³⁷X. Chen, J. Zhao, G. Wang, and X. Shen, *Phys. Lett. A* **212**, 285 (1996).
- ³⁸O. Madelung, *Semiconductors: Data Handbook* (Springer, Berlin, 2004).
- ³⁹A. D. Yoffe, *Adv. Phys.* **42**, 173 (1993).
- ⁴⁰R. D. Schaller, V. M. Agranovich, and V. I. Klimov, *Nat. Phys.* **1**, 189 (2005).
- ⁴¹N. Turaeva, B. Oksengendler, and I. Uralov, *Appl. Phys. Lett.* **98**, 243103 (2011).
- ⁴²O. Christensen, *J. Appl. Phys.* **47**, 689 (1976).
- ⁴³A. J. Nozik, *Annu. Rev. Phys. Chem.* **52**, 193 (2001).
- ⁴⁴M. T. Trinh, A. J. Houtepen, J. M. Schins, T. Hanrath, J. Piris, W. Knulst, A. P. L. M. Goossens, and L. D. A. Siebbeles, *Nano Lett.* **8**, 1713 (2008).
- ⁴⁵G. Allan and C. Delerue, *Phys. Rev. B* **73**, 205423 (2006).
- ⁴⁶M. C. Beard, A. G. Midgett, M. C. Hanna, J. M. Luther, B. K. Hughes, and A. J. Nozik, *Nano Lett.* **10**, 3019 (2010).
- ⁴⁷Y. Kayanuma, *Phys. Rev. B* **38**, 9797 (1988).
- ⁴⁸G. Nair, S. M. Geyer, L. Y. Chang, and M. G. Bawendi, *Phys. Rev. B* **78**, 125325 (2008).
- ⁴⁹J. A. McGuire, J. Joo, J. M. Pietryga, R. D. Schaller, and V. I. Klimov, *Acc. Chem. Res.* **41**, 1810 (2008).
- ⁵⁰V. I. Klimov, *Annu. Rev. Phys. Chem.* **58**, 635 (2007).
- ⁵¹M. C. Hanna and A. J. Nozik, *J. Appl. Phys.* **100**, 074510 (2006).
- ⁵²G. Nair, L. Y. Chang, S. M. Geyer, and M. G. Bawendi, *Nano Lett.* **11**, 2145 (2011).
- ⁵³W. Shockley and H. J. Queisser, *J. Appl. Phys.* **32**, 510 (1961).
- ⁵⁴M. Razeghi and A. Rogalski, *J. Appl. Phys.* **79**, 7433 (1996).